JOURNAL OF AGRICULTURAL AND FOOD CHEMISTRY

Article

pubs.acs.org/JAFC

Lipidomic Fingerprint of Almonds (*Prunus dulcis* L. cv Nonpareil) Using TiO_2 Nanoparticle Based Matrix Solid-Phase Dispersion and MALDI-TOF/MS and Its Potential in Geographical Origin Verification

Qing Shen,[†,∥] Wei Dong,[†,∥] Mei Yang,[†] Linqiu Li,[†] Hon-Yeung Cheung,*[,†] and Zhifeng Zhang*[,‡]

[†]Department of Chemistry and Biology, City University of Hong Kong, Tat Chee Avenue, Kowloon, Hong Kong SAR, China

[‡]Ethnic Pharmaceutical Institute, Southwest University for Nationalities, Chengdu, Sichuan Province, China

ABSTRACT: A matrix solid-phase dispersion (MSPD) procedure with titanium dioxide (TiO_2) nanoparticles (NP) as sorbent was developed for the selective extraction of phospholipids from almond samples, and matrix-assisted laser desorption ionization−time-of-flight mass spectrometry (MALDI-TOF/MS) was employed for analysis. A remarkable increase in the signals of phospholipid accompanied by a decrease in those of triacylglycerols and diacylglycerols was observed in the relevant mass spectra. The proposed method was applied to five batches of almonds originating from four geographical areas, whereas principal component analysis (PCA) was utilized to normalize the relative amounts of the identified phospholipid species. The results indicated that the lipidomic fingerprint of almonds was successfully established by the negative ion mode spectrum, and the ratio of m/z 833.6 to 835.6 as well as m/z 821.6 could be introduced as potential markers for the differentiation of the tested almonds with different geographical origins. The whole method is of great promise for selective separation of phospholipids from nonphospholipids, especially the glycerides, and superior in fast screening and characterization of phospholipids in almond samples.

KEYWORDS: *lipidomic fingerprint, TiO_2, matrix solid-phase dispersion, principal component analysis, MALDI-TOF/MS, almond*

INTRODUCTION

Almonds are the seeds of *Prunus dulcis*, an ancient crop of Western and Central Asia.[1] The kernel, encased in a brown leathery seed coat, is commonly utilized in bakery and confectionary items, such as cereals, snack formulations, and marzipan.[2,3] As one of the few alkaline nuts, almonds are widely used in ayurvedic medicine in the relief of phlegm and coughs, lubrication of the intestines, and growth inhibition of cancer cells.[4] Meanwhile, significant improvements in learning and memory as well as decreases in plasma cholesterol level have been noted in rats treated with almond.[5] The health effects are generally attributed to the polyunsaturated lipids, choline, and phenolic compounds in almonds.[6] Current published studies focused mainly on the composition and effects of phenolic compounds,[7] but studies on the lipid profile are relatively scarcer. It is also worth mentioning that the quality of almond depends simultaneously on the genotype and the exogenous conditions.[8−10] There are a lot of methods developed for almond cultivar characterization, such as high-performance liquid chromatography (HPLC),[11] inductively coupled plasma (ICP),[12] gas chromatography−mass spectrometry (GC-MS),[13] infrared spectroscopy (IR),[14] and thermal analysis techniques,[15] but a method for differentiating geographical origins is still lacking.

In biochemical, physiological, and nutritional studies, there are increasing considerations of phospholipids as nutrients with putative health benefit effects. Phospholipids play vital biological roles in lipid digestion, absorption, and transport, in inflammatory processes, and in signaling pathways as essential components of the lipid bilayer of cell membranes.[16] Phospholipids show complicated molecular types due to a glycerol backbone with one headgroup at the sn-3 position and a fatty acid substituent at the sn-1 and/or sn-2 position. Research works have been conducted and indicated that some species of phospholipids could be regarded as potential markers for monitoring adulteration, detecting food rancidity, and differentiating species; for example, Calvono et al. have introduced phospholipids as markers for monitoring illegal milk and olive oil adulteration.[17,18] Wang et al. monitored the dynamic changes of phospholipids for detecting fish rancidity during storage.[19] Phospholipids were also widely used as markers for fish species differentiation.[20−22]

The rapid development of the research field of lipidomics is driven by the rapid advances in technologies such as HPLC, MS, nuclear magnetic resonance (NMR) spectroscopy, fluorescence spectroscopy, MALDI imaging MS, and computational methods.[23−27] These techniques are efficient in recognizing the role of lipids in many metabolic diseases such as obesity, ankylosing spondylitis, hypertension, diabetes, and cardiovascular disease.[28,29] In addition, titanium dioxide (TiO_2) based material facilitated sample preparation of compounds with a phosphoryl group, including phosphopeptides and phospholipids, due to the selective interaction between the phosphate group and TiO_2 surface by a chelating bidentate bond.[30] Calvano et al. have recently illustrated that efficient and selective phospholipid enrichment can be achieved from dairy products using solid-phase extraction by homemade micro-

Received: April 16, 2013
Revised: July 22, 2013
Accepted: July 22, 2013
Published: July 22, 2013

ACS Publications © 2013 American Chemical Society

columns packed with (TiO_2) microparticles (4.0 mm diameter).[31]

The objective of this study was to develop a simple procedure for the selective extraction of phospholipids from complex almond samples based on matrix solid-phase dispersion with TiO_2 nanoparticles (NPs) as sorbent. The fortified phospholipid samples were further subjected to fast MALDI-TOF/MS for fingerprinting. The overall method was optimized and then applied to identify almonds from different geographical origins.

MATERIALS AND METHODS

Materials. Four batches of almonds (*P. dulcis* L. cv Nonpareil) were bought from Turpan (China), Yunzhou (China), New Delhi (India), and California (USA). Almond (*P. dulcis* var. *amara*) was also bought from Turpan (China). All of the samples were authenticated by Prof. Hao Zhang (School of Pharmacy, Sichuan University) and deposited in the Laboratory of Natural Products, City University of Hong Kong (No. 320081, 320082, 320083, 320084, and 320085). For preparation, the almonds (kernels with seed coat) were ground into powder and screened through a sieve with particle size of <250 μm before extraction. 2,5-Dihydroxybenzoic acid (DHB) was purchased from Sigma-Aldrich (St. Louis, MO, USA) and dissolved in methanol with a final concentration of 30 mg/mL as stock solution. HPLC grade chloroform and methanol were purchased from Fisher Scientific (Waltham, MA, USA). Water with a resistivity of 18 MΩ cm^{-1} was purified using a Milli-Q system from Millipore (Billerica, MA, USA).

TiO_2 NP Based MSPD. Approximately 1 g of homogenized almond powder was weighed and transferred into a glass mortar. The extraction sorbent, TiO_2 NP, was added to the same mortar at a sample/sorbent mass ratio of 1:2. The mixture was ground thoroughly by a glass pestle for approximately 10 min until a fine powder was obtained. About 100 mg of the sample powder was packed into the cartridge, where a 2 mm polypropylene lower frit was fixed at the bottom. In front of the cartridge, another polypropylene frit was introduced to fix the stationary phase, which is a bed of TiO_2 NPs of 0.8 cm in height. The packed column was gently tapped to remove the trapped air. During the extraction process, the TiO_2 NP packed cartridge was washed with 3 mL of acidified water (pH 5) and eluted by binary solvent mixtures of chloroform and methanol (1:2). The flow speed was controlled at 1−2 drops/s by the Teflon clog.

Bligh and Dyer (B&D) Method. For each sample, 1.0 g of powder was added to 1.75 mL of binary solvent mixture of chloroform and methanol (1:2) and vortexed well. Then, 1.25 mL of chloroform was added, followed by sonication extraction using an ultrasonic cleaning device for 15 min. Finally, an aliquot of 1.25 mL of water was added for the separation of the phase. After centrifugation at 8000 rpm for 10 min, the lower organic phase was recovered and transferred to a new glass tube by pipet. The aqueous phase was re-extracted with 2.0 mL of chloroform another two times as described before. The collected organic phases were combined and evaporated under nitrogen flow.

MALDI Spotting. For MALDI analysis, the procedure for sample preparation is analogous to the sandwich method that is commonly used in MALDI-TOF/MS. To optimize the lipidomic fingerprinting method, the extracts of almond samples were spotted onto the MALDI target. After water evaporation, a thin layer (0.3 μL) of matrix solution was then spotted on the dried sample. After the evaporation of the matrix solvent, the samples were ready to be directly analyzed by MALDI-TOF/MS.

MALDI Mass Spectrometry. All mass spectra shown were obtained using an Applied Biosystems 4800 MALDI-TOF/TOF mass spectrometer (AB Sciex, Foster City, CA, USA) equipped with a 200 Hz triple-frequency Nd:YAG pulsed laser with 355 nm wavelength. Measurements were performed either in positive or negative ion reflection mode at an accelerating potential of 20 kV. A delayed ion extraction time of 450 ns was selected according to the mass range under observation (m/z 450−1000) allowing for baseline isotopic mass resolution. Mass spectra were obtained by applying laser energy adjusted to 5−10% above threshold irradiation according to the manufacturer's nominal scale. An integrated video imaging system (~25× magnification) allowed direct observation of the sample spots under investigation. External mass calibration was achieved using a mixture of phospholipid standard compounds described above. MS data acquisition was performed by 4000 Series Explorer, version 3.5.2 program.

Data Analysis. MALDI-MS/MS data analysis was performed by the supplied instrument software Data Explorer v.4.9 (Applied Biosystems) using the Savitzky−Golay smoothing algorithm. Lipid characterization was performed by comparing accurate mass measurements with the LIPID MAPS prediction tool (http://www.lipidmaps.org/tools/index.html) and confirmed by MS/MS in LIFT-TOF/TOF mode. Values were displayed as the mean ± standard deviation (SD) of at least triplicate measurements ($n \geq 3$). Principal component analysis (PCA) was applied to determine the main sources of variability present in the data sets and to establish the relationship between samples (objects) and phospholipids (variables). The raw data were imported into the statistical software package MarkerView, version 1.2.1 (AB Sciex, Concord, Canada), and the software would look for the difference in the mass fragments (m/z) and the relative abundance.

RESULTS AND DISCUSSION

MSPD Optimization. TiO_2 was selected as sorbent for selective extraction of phospholipids, because it has already proved the electrostatic interactions between the phosphoryl group and the positively charged TiO_2 surface.[32] The sample-to-sorbent ratio and the suitability of the extraction solvent are the two major factors that influence the efficiency of the extraction and the cleanness of the final extracts. Therefore, the MSPD optimization was carried out by sequential selection of the sample-to-sorbent ratio, cleanup, and eluting solvents to achieve extracts with the highest recovery and the lowest effects of matrix interferences from the almond samples.

The first series of experiments was the evaluation of a suitable sample-to-sorbent ratio to allow complete adsorption of the almond components and to facilitate the transfer into the cartridge. Ratios varying from 1:1 to 1:4 have been selected depending on the nature of the sample. To verify whether optimum conditions were achieved, different amounts of TiO_2 NPs (1, 2, and 4 g) were added to the glass mortar and blended with 1 g of sample, and then the elution was performed as described before. In this study, the ratio of 1:2 was found to be satisfactory for proper dispersion of samples, and no further improvement in extraction efficiency was observed with increasing sorbent percentage. Furthermore, reduction of the ratio to 1:1 resulted in maximal errors during analysis, which might be induced by the fact that the cartridge packing material was not as homogeneous as required.

An appropriate washing solvent should efficiently retain the target analytes on the sorbent and remove interferential matrices from the cartridge. Studies on molecules containing phosphonate or phosphate moieties have shown that under acidic pH, these groups confer high affinity to TiO_2, and the most favorable bonding mode is bidentate, involving two oxygen atoms in each bond.[32] Therefore, acidified water was applied, not only to remove the polar compounds but also to enhance the binding ability of the TiO_2 NP sorbent. The removal of the highly water-soluble pigments could be directly observed during the washing process. In addition, acetone and hexane were investigated as washing solvents to eliminate the abundant glycerides contained in almond samples. For this purpose, the acidified cartridge was further washed by hexane and acetone individually. The results indicated that acetone

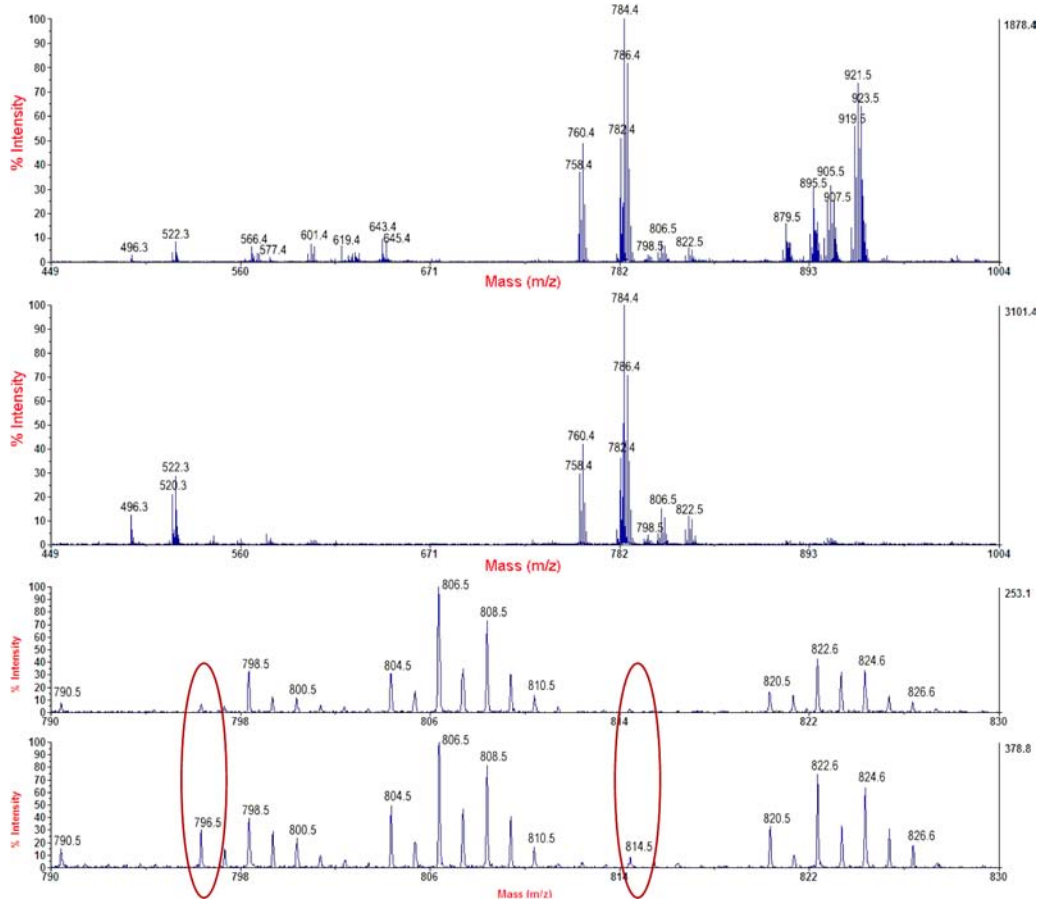

Figure 1. MALDI MS spectra relevant to the extracts of almond samples by B&D method (A, top) and TiO_2 NPs based MSPD method (B, middle) in positive ion mode; zoom of the m/z range 790−830 for the spectra of B&D method (C, bottom) and TiO_2 NPs based MSPD method (D).

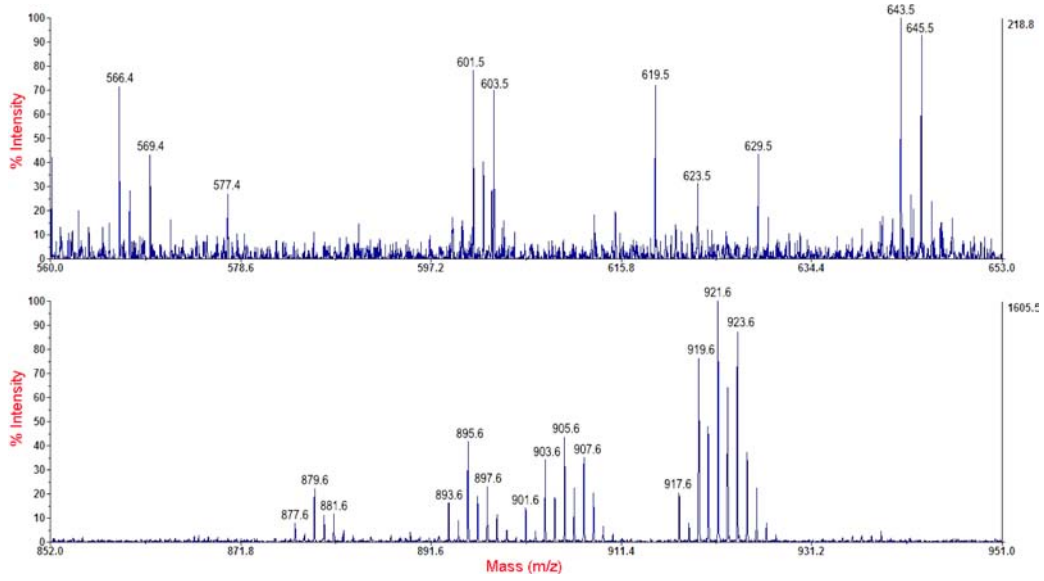

Figure 2. Expanded views of the m/z ranges 530−650 (A, top) and 850−950 (B, bottom) of the spectra reported in Figure 1A, to show the DAG and TAG species, respectively.

showed better performance than hexane because a cleaner spectrum was observed. On the basis of these results, 3 mL of acidified water at pH 5 and 3 mL of acetone were utilized.

Except for the washing step, the nature of the elution solvent should also be taken into consideration, because the target analytes should be efficiently desorbed, whereas the remaining matrix components should be retained in the cartridge. The classic mixture of dichloromethane and methanol was tested as elution solvent, and its polarity strength was adjusted by varying the ratio of dichloromethane to methanol from 2:1 to 1:2. The

dx.doi.org/10.1021/jf4016448 | J. Agric. Food Chem. 2013, 61, 7739−7748

results indicated that the binary solvent mixture of dichloromethane and methanol (1:2) gave the highest extraction efficiency for phospholipids.

Lipid Characterization and Method Comparison. In the present study, DHB was employed because it is readily soluble in organic solvents, thus enhancing the homogeneity of crystallization of the sample and matrix mixture and leading to reproducible MALDI-TOF/MS measurements and well-resolved mass spectra. An isotopic correction was performed to ensure that minor peaks were not the result of isotopic distribution of the adjacent and more dominant lipid peaks.

Positive Ion Mode. The B&D method was used as starting point because it proved to extract the phospholipids more efficiently than the nonpolar lipids. The lipid profile of almond is illustrated in Figure 1A in a clear and systematic manner. The ions in the m/z 850−950 range corresponding to TAG were detected mainly as their potassium adducts, that is, $[TAG + K]^+$. Minor ions of $[TAG + Na]^+$ were also detected but in comparatively lower intensities. The ions detected in the m/z 550−650 range corresponded mostly to $[DAG + K/Na]^+$ and fragments from $[TAG + K/Na]^+$ ions because of the loss of a fatty acyl moiety. Figure 2 shows a zoomed-in view of Figure 1A, the typical spectra of DAG region (A) and TAG region (B) of the MALDI-TOF/MS, whereas Table 1 summarizes the

Table 1. Attribution of the Main Ions Observable in the Spectra of Figures 1A and 2

mass (m/z)	probable attribution[a]		
569.4	$[PP + H]^+$		
577.4	fragment $[PO]^+$		
601.5	fragment $[OL]^+$		
603.5	fragment $[OO]^+$		
619.5	$[PS + Na]^+$		
623.5	$[SO + H]^+$		
629.5	$[PtLn + K]^+$		
643.5	$[OO + Na]^+$		
645.5	$[SO + Na]^+$		
877.6	$[LLLn + H]^+$	$[PLL + Na]^+$	$[POLn + Na]^+$
879.6	$[LLL + H]^+$	$[OLLn + H]^+$	$[POL + Na]^+$
881.6	$[OLL + H]^+$	$[OOLn + H]^+$	$[POO + Na]^+$
893.6	$[PLL + K]^+$	$[POLn + K]^+$	
895.6	$[POL + K]^+$		
897.6	$[POO + K]^+$	$[PSL + K]^+$	
901.6	$[LLL + Na]^+$		
903.6	$[OLL + Na]^+$		
905.6	$[OOL + Na]^+$		
907.6	$[OOO + Na]^+$	$[SOL + Na]^+$	
909.6	$[SOO + Na]^+$	$[SSL + Na]^+$	
917.6	$[LLL + K]^+$		
919.6	$[OLL + K]^+$		
921.6	$[OOL + K]^+$	$[SLL + K]^+$	
923.6	$[OOO + K]^+$	$[SOL + K]^+$	

[a]M, myristic acid (14:0); P, palmitic acid (16:0); Pt, palmitoleic acid (16:1); O, oleic acid (18:1); S, stearic acid (18:0); L, linoleic acid (18:2); Ln, linolenic acid (18:3).

glyceride composition profiles as determined from these spectra. In the DAG mass range (Figure 2A), the dominate ions identified were $[SO + Na]^+$ (m/z 645.5), $[OO + Na]^+$ (m/z 643.5), $[PtLn + K]^+$ (m/z 629.5), $[SO + H]^+$ (m/z 623.5), $[PS + Na]^+$ (m/z 619.5), and $[PP + H]^+$ (m/z 569.4). It was noted that the ions of m/z 577.4, 601.5, and 603.5 corresponded to fragment ions $[PO]^+$, $[OL]^+$, and $[OO]^+$, respectively. The dominant peaks identified in the TAG region (Figure 2B) were these of potassium-adducted TAG compositions $[OLL + K]^+$ (m/z 919.6), $[OOL + K]^+/[SLL + K]^+$ (m/z 921.6), and $[OOO + K]^+/[SOL + K]^+$ (m/z 923.6), as well as sodiated ones $[LLL + Na]^+$ (m/z 901.6), $[OLL + Na]^+$ (m/z 903.6), $[OOL + Na]^+$ (m/z 905.6), $[OOO + Na]^+/[SOL + Na]^+$ (m/z 907.6), and $[SOO + Na]^+/[SSL + Na]^+$ (m/z 907.6). The other main peaks identified were attributed to the compositions $[PLL + K]^+/[POLn + K]^+$ (m/z 893.6), $[POL + K]^+$ (m/z 895.6), $[POO + K]^+/[PSL + K]^+$ (m/z 897.6), $[LLLn + H]^+/[PLL + Na]^+/[POLn + Na]^+$ (m/z 877.6), $[LLL + H]^+/[OLLn + H]^+/[POL + Na]^+$ (m/z 879.6), and $[OLL + H]^+/[OOLn + H]^+/[POO + Na]^+$ (m/z 881.6).

Phospholipids were another important lipid group detected in this experiment in abundant amounts. On the basis of MS/MS data and the literature and with the help of database LIPID MAPS, the peaks observed in the m/z range 750−850 corresponding to phospholipids and those in the m/z range 450−550 corresponding to lysophospholipids were identified and summarized in Table 2. Potassium/sodium adducted PC species were the main detected ions, whereas PE species were also detected in minor abundance. The exclusive detection of PC is not surprising because lipids with quaternary ammonia groups are particularly detectable due to the permanent positive charge of these groups. PC species with moderately unsaturated oleic acyl and linoleic acyl residues dominated the spectrum, mainly m/z 782.4, 784.4, and 786.4, corresponding to $[PC18:2/18:2 + H]^+$ and $[PC16:0/18:1 + Na]^+$, $PC18:1/18:2 + H]^+$, and $[PC18:0/18:2 + H]^+$ and $[PC18:1/18:1 + H]^+$, respectively. The other main peaks identified were attributed to the compositions $[PC16:0/18:2 + H]^+$ (m/z 758.4), $[PC16:0/18:1 + H]^+$ (m/z 760.4), $[PC18:1/18:2 + Na]^+$ (m/z 806.5), and $[PC18:1/18:2 + K]^+$ (m/z 822.5). Some lysophospholipids were also observed such as the ions of m/z 496.3, 520.3 and 522.3, corresponding to $[LPC16:0 + H]^+$, $[LPC18:2 + H]^+$, and $[LPC18:1 + H]^+$, respectively. No highly unsaturated fatty acyl residues such as docosahexaenoyl (22:6) and eicosapentaenoyl (20:5) can be detected, which is a major difference from aquatic organisms.

A representative mass spectrum of almond using the TiO_2 NP based MSPD method is shown in Figure 1B. Comparison of panels A and B of Figure 1 indicated that the nonphospholipid ions including DAG, TAG, and their fragments disappeared, whereas ions of phospholipids were well preserved and clearly observed. Meanwhile, the intensity of the signals increased up to approximately 2 times. Panels C and D of Figure 1 show the expanded views of the m/z range 790−830 of the spectra reported in Figure 1A,B, respectively. Apparently, the TiO_2 NP based MSPD method produced more informative results. For example, the m/z ion of 796.5 corresponding to $[PE18:1/20:0 + Na]^+$ was almost absent in the spectrum of B&D extracts, whereas in the spectrum of the new extraction approach, the m/z ion 796.5 was clearly observed. In general, when the traditional B&D method was used, the formation of glycerol ions suppressed the sensitivity for the detection of phospholipid due to the in-source competition of ionization, which is one of the major obstacles for the reliable quantitative evaluation of MALDI mass spectra of phospholipids derived from complex samples. These data confirm a great increase in selectivity and extraction efficiency toward phospholipids when using TiO_2 as sorbent for MSPD.

Table 2. Attribution and Relative Amount of the Main Phospholipid Ions in Five Almond Samples

mass (m/z)	probable attribution	geographic origins				
		Turpan[a]	Yunzhou[a]	New Delhi[a]	California[a]	Turpan[b]
	Positive Ion Mode					
496.3	$[LPC16:0 + H]^{+}$[c]		1.71		1.08	
518.4	$[LPC18:3 + H]^{+}$		0.42			
520.4	$[LPC18:2 + H]^{+}$	0.93	3.02	0.8	1.27	0.6
522.4	$[LPC18:1 + H]^{+}$	2.82	4.41	1.78	4.5	1.93
542.4	$[LPC18:2 + Na]^{+}$		0.31	0		
544.4	$[LPC18:1 + Na]^{+}$	0.19	0.4	0.5	0.59	0.37
558.4	$[LPC18:2 + K]^{+}$		0.26			
560.4	$[LPC18:1 + K]^{+}$	0.23	0.31	0.4	0.66	0.31
732.5	$[PC16:0/16:1 + H]^{+}$	0.22	0.25		0.21	
734.5	$[PC16:0/16:0 + H]^{+}$		0.28			
742.5	$[PE18:1/18:2 + H]^{+}$			0.41	0.28	0.33
744.5	$[PE18:0/18:2 + H]^{+}$, $[PE18:1/18:1 + H]^{+}$			0.31	0.18	0.27
756.5	$[PC16:1/18:2 + H]^{+}$, $[PC16:0/18:3 + H]^{+}$		0.29	0.65		
758.5	$[PC16:0/18:2 + H]^{+}$	3.78	7.23	6.52	2.42	3.17
760.5	$[PC16:0/18:1 + H]^{+}$	11.21	8.98	12.39	7.69	9.37
780.5	$[PC18:2/18:3 + H]^{+}$, $[PC16:0/18:2 + Na]^{+}$	1.26	1.46	1.34	0.29	0.44
782.5	$[PC18:2/18:2 + H]^{+}$, $[PC16:0/18:1 + Na]^{+}$	6.05	10.13	9.43	3.28	3.62
784.5	$[PC18:1/18:2 + H]^{+}$	22.04	23.01	28.35	15.74	18.7
786.5	$[PC18:0/18:2 + H]^{+}$, $[PC18:1/18:1 + H]^{+}$	36.32	14.68	32.77	39.52	37.26
788.5	$[PC18:0/18:1 + H]^{+}$	2.15	1.07	0.88	1.66	0.36
796.5	$[PE18:1/20:0 + Na]^{+}$		0.65	0.68	0.35	0.46
798.5	$[PE18:1/22:2 + H]^{+}$, $[PE18:0/20:0 + Na]^{+}$	1.04	0.96	1.6	1.11	1.59
800.5	$[PE18:1/22:1 + H]^{+}$, $[PE18:0/22:2 + H]^{+}$	0.74	0.27	0.96	0.87	0.64
804.5	$[PC18:2/18:2 + Na]^{+}$	0.57	1.27	1.26		0.22
806.5	$[PC18:1/18:2 + Na]^{+}$	3.28	3.13	3.95	1.5	2.16
808.5	$[PC18:0/18:2 + Na]^{+}$, $[PC18:1/18:1 + Na]^{+}$	5.49	1.99	4.08	3.59	3.57
810.5	$[PC18:0/18:1 + Na]^{+}$		0.1	0.31	0.03	0.18
814.5	$[PC18:1/20:1 + H]^{+}$		0.24			
820.5	$[PC18:2/18:2 + K]^{+}$		0.78	0.8	0.38	0.41
822.6	$[PC18:1/18:2 + K]^{+}$	1.92	1.56	4.25	2.04	2.69
824.6	$[PC18:0/18:2 + K]^{+}$, $[PC18:1/18:1 + K]^{+}$	2.95	1.07	4.02	4.73	5.23
826.6	$[PC18:0/18:1 + K]^{+}$		0.1	0.25	0.18	0.18
	Negative Ion Mode					
571.4	$[PI16:0 - H]^{-}$	1.01	3.26	1.68	0.25	
595.4	$[PI18:2 - H]^{-}$	0.48	0.77	2.00	1.87	
597.4	$[PI18:1 - H]^{-}$	2.48	1.45	2.55	2.6	1.2
599.4	$[PI18:0 - H]^{-}$		0.47		0.93	
698.4	$[PE\ O - 16:0/18:3 - H]^{-}$/$[PE\ O - 16:1/18:2 - H]^{-}$	0.67				
699.4	$[PA18:0/18:2 - H]^{-}$, $[PA18:1/18:1 - H]^{-}$	0.39	0.64	0.73	0.55	1.57
716.5	$[PE16:0/18:1 - H]^{-}$/$[PE16:1/18:0 - H]^{-}$	0.57	0.28	0.57		1.49
725.5	$[PA18:1/20:2-H]^{-}$, $[PA18:2/20:1-H]^{-}$	1.01	1.17	1.29	1.29	0.92
740.5	$[PE18:1/18:2 - H]^{-}$, $[PC16:1/18:2 - CH_3]^{-}$	0.98	0.76	0.5		1.24
741.5	$[PG16:1/18:3 - H]^{-}$	0.37	0.48		1.12	
742.5	$[PE18:1/18:1 - H]^{-}$, $[PC16:0/18:2 - CH_3]^{-}$	1.28	1.47	1.79	1.73	2.68
744.5	$[PE18:0/18:1 - H]^{-}$, $[PC16:0/18:1 - CH_3]^{-}$	2.27	2.18	1.82	1.28	2.29
745.5	$[PG16:0/18:2 - H]^{-}$, $[PG16:1/18:1 - H]^{-}$	0.29	0.19			0.76
747.5	$[PG16:0/18:1 - H]^{-}$	0.77	0.28			0.32
749.5	$[PG16:0/18:0 - H]^{-}$	0.47		0.55		
751.5	$[PA18:0/22:4 - H]^{-}$, $[PA18:2/22:2 - H]^{-}$	1.01	0.41	0.79		0.45
766.5	$[PE18:1/20:3 - H]^{-}$, $[PE18:2/20:2 - H]^{-}$, $[PC18:2/18:2 - CH_3]^{-}$	1.00	0.99	0.39		0.28
767.5	$[PG18:2/18:3 - H]^{-}$	0.32		0.31		
768.5	$[PE18:1/20:2 - H]^{-}$, $[PE18:2/20:1 - H]^{-}$, $[PC18:1/18:2 - CH_3]^{-}$	2.73	3.37	1.25	3.72	3.48
769.5	$[PG18:2/18:2 - H]^{-}$	0.48	0.47	0.23	0.3	1.44
770.5	$[PE18:1/20:1 - H]^{-}$, $[PE18:2/20:0 - H]^{-}$, $[PC18:0/18:2 - CH_3]^{-}$, $[PC18:1/18:1 - CH_3]^{-}$	4.72	2.82	2.76	6.66	4.06
818.6	uc[d]		0.87	0.59	1.45	
820.6	uc	1.47	0.56	0.67	1.55	1.67
821.6	$[PI\ O - 16:0/18:1 - H]^{-}$				1.14	

dx.doi.org/10.1021/jf4016448 | J. Agric. Food Chem. 2013, 61, 7739−7748

Table 2. continued

mass (m/z)	probable attribution	geographic origins				
		Turpan[a]	Yunzhou[a]	New Delhi[a]	California[a]	Turpan[b]
	Negative Ion Mode					
831.6	$[PI16:1/18:2 - H]^-$	0.54	1.11	0.76		
833.6	$[PI16:0/18:2 - H]^-$, $[PI16:1/18:1 - H]^-$	11.54	28.73	24.16	11.23	11.71
835.6	$[PI16:0/18:1 - H]^-$	25.36	15.06	22.23	23.89	25.37
857.6	$[PI16:0/18:0 - H]^-$	1.18	1.15	0.78		0.75
859.6	$[PI18:0/18:3 - H]^-$, $[PI18:1/18:2 - H]^-$	5.75	4.38	4.8	4.77	3.87
861.6	$[PI18:0/18:2 - H]^-$, $[PI18:1/18:1 - H]^-$	15.11	5.78	9.33	15.57	9.58
863.6	$[PI18:0/18:1 - H]^-$	4.33	2.37	3.83	4.24	1.05
865.6	$[PI18:0/18:0 - H]^-$	0.24				0.94

[a]*Prunus dulcis* L. cv Nonpareil. [b]*Prunus dulcis* var. *amara*. [c]The LPL or PL molecular species are shown by the format of A B:C/D:E, where A represents the phospholipid classes, B represents the number of total carbon atoms of the fatty acyl chain (sn1), C represents the number of total double bonds of the fatty acyl chain (sn1), D represents the number of total carbon atoms of the fatty acyl chain (sn2), and E represents the number of total double bonds of the fatty acyl chain (sn2). LPC, lysophosphatidylcholine; PC, phosphatidylcholine; PE, phosphatidylethanolamine; PI, phosphatidylinositol; PA, phosphatidic acid; PG, phosphatidylglycerol. [d]Uncertain.

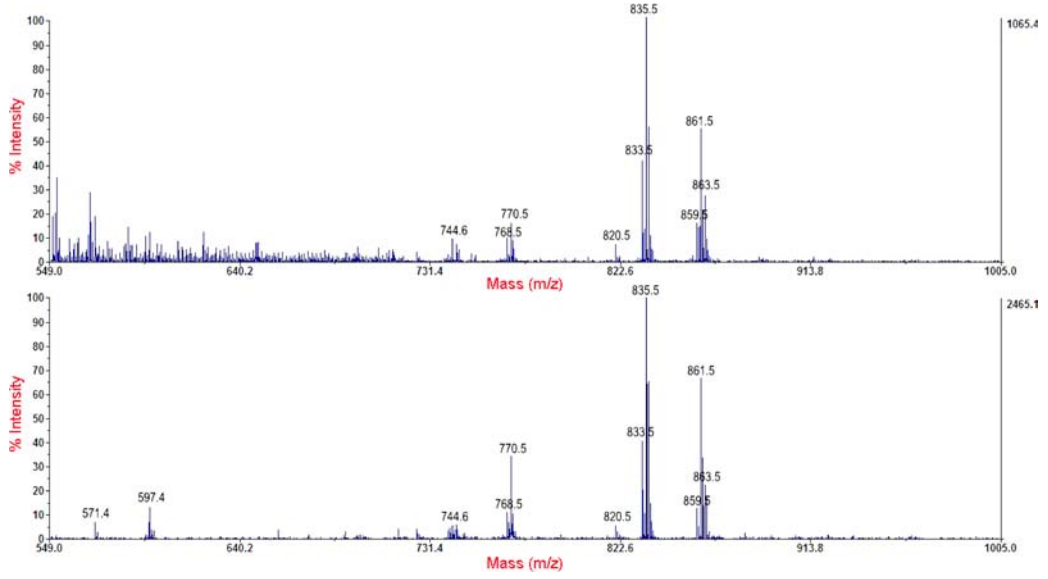

Figure 3. MALDI MS spectra relevant to the extracts of almond samples by B&D method (A, top) and TiO_2 NPs based MSPD method (B, bottom) in negative ion mode.

Negative Ion Mode. Negative ion mode was also conducted, and the spectra are shown in Figure 3. In fact, the negative ion mode is used to facilitate the detection of acidic phospholipids, which yield mainly negative ions, in samples with excess PC or sphingomyelin. Figure 3 shows the negative spectra of lipid extracts using the B&D method (A) and the TiO_2 NP based MSPD method (B). Both spectra show more diversity than that of positive ion mode, because some phospholipids are more sensitively and accurately detected as negative ions, such as the classes of PI, PG, PA, and PE. In negative ion mode, PI was found to be the most abundant class of phospholipid, accounting for 58−80% of the total. The dominant ions in the mass range 830−870 were all identified as PI species, for instance, $[PI16:0/18:2 - H]^-$/$[PI16:1/18:1 - H]^-$ (m/z 833.6), $[PI16:0/18:1 - H]^-$ (m/z 835.6), $[PI18:0/18:3 - H]^-$/$[PI18:1/18:2 - H]^-$ (m/z 859.6), $[PI18:0/18:2 - H]^-$/$[PI18:1/18:1 - H]^-$ (m/z 861.6), and $[PI18:0/18:1 - H]^-$ (m/z 863.6). PC and PE species ranked second, accounting for 9−15%. It is worth mentioning that abundant $[M - 15]^-$ peaks of PC species can also be generated by the negative ion mode of MALDI-TOF/MS, overlapping with $[M - H]^-$ ions of PE species within the mass range of 700−850 Da when crude phospholipids are directly spotted into the MALDI plate without LC separation of lipid classes. For example, the ions of $[PE18:1/20:2-H]^-$, $[PE18:2/20:1-H]^-$, and $[PC18:1/18:2-CH_3]^-$ were overlapped at m/z 768.5. PA and PG were the minor classes, accounting together for <10% of the total phospholipids. The low level of PA may be attributed to its function as a signaling molecule or its conversion to triglycerides, whereas the low level of PG may because of the suppression of PG synthesis by PI synthesis from phosphatidate via cytidine diphosphate−-diacylglycerol myoinositol phosphatidyltransferase.[33] By comparing panels A and B of Figure 3, it could be observed that the complicated B&D extracts resulted in the ion suppression effect in MALDI ionization and numerous significant background peaks within the low mass range (m/z 550−700, Figure 3A), with the contribution of botanical small molecules. As shown apparently, the negative spectrum of the same almond extract but using TiO_2 NP based MSPD method was cleaner and the signals were much more

dx.doi.org/10.1021/jf4016448 | J. Agric. Food Chem. 2013, 61, 7739−7748

intense, making relative quantitation achievable. Especially in the low mass range 550−600, ions of m/z 571.4, 595.4, 597.4, and 599.4 were detectable and identified as $[LPI16:0 - H]^-$, $[LPI16:0 - H]^-$, $[LPI16:0 - H]^-$, and $[LPI16:0 - H]^-$, respectively.

Method Application and Data Analysis. The TiO_2 NP based MSPD together with MALDI-TOF/MS method was applied to analyze five batches of almonds (12 samples for each batch) from four different geographical origins, including Turpan (China), Yunzhou (China), New Delhi (India), and California (USA). The results are summarized in Table 2. The relative amounts of individual phospholipid species vary greatly because the occurrence of phospholipids is easily influenced by environmental stresses, such as temperature, nutrient supply, light, and age.[34]

To identify the difference of phospholipid species between the almond samples, principal component analysis (PCA) was applied to normalize the relative amounts of the identified phospholipid species and the overall almond samples (12 for each batch) in a reduced-dimension plot. PCA is a powerful statistical analytical technique used for explaining the variance of a large set of intercorrelated variables (phospholipid species) and transforming them into a smaller set of uncorrelated variables, namely, principal components (PC). The first two PCs were extracted explaining 57.9 cumulative percent (cum %) value of the total variance of the data set, where PC1 explains 41.6 cum % of the variance in the initial data set and PC2 explains 16.3 cum %. As seen in Figure 4A, the first principal component (PC1) is plotted against the second (PC2), and the distribution of the samples implies that the Yunzhou and New Delhi almonds were significantly different from other batches. The California batch could be distinguished with satisfactory PCA performance, whereas both *P. dulcis* L. cv Nonpareil and *P. dulcis* var. *amara* of the Turpan batch were overlapped in the PCA plot.

Furthermore, the coefficient that defines the weight of the original variable in the PC was investigated to understand which phospholipid species are responsible for the diversity of the samples. The study of loadings for the variables in the first two principal components is shown in Figure 4B. The phospholipids that explain maximum variance in the data had higher loading values, whereas others that do not play an important role provided loading values near 0. This shows that m/z 833.6, 782.5, 835.6, and 786.5 were the dominant features in the first principal component with loading values of −0.47, −0.20, 0.28, and 0.52, respectively. Meanwhile, the loading values of m/z 760.5, 835.6, 786.5, and 784.5 were 0.30, 0.30, 0.30, and 0.49, respectively, which were the main contributors in PC2. This indicated that these kinds of ions could be used as potential markers for the differentiation of each almond batches.

On the basis of the PCA results, the characteristic ions in PC1 that accounted for more cumulative percentage were further inspected and discussed. First, the ions of m/z 833.6 and 835.6 were studied by expanded views of the m/z range 820−870 of negative spectra of almonds from different geographical origins (Figure 5). It could be observed that the difference in the composition between Yunzhou, New Delhi, and the other three batches was remarkable. The Yunzhou almond batch contained the highest relative amount of $[PI34:2 - H]^-$ (m/z 833.6) and the ratio to $[PI34:1 - H]^-$ (m/z 835.6) was 1.91, significantly higher than that of the rest of the almond samples. For the New Delhi samples, the ratio of m/z

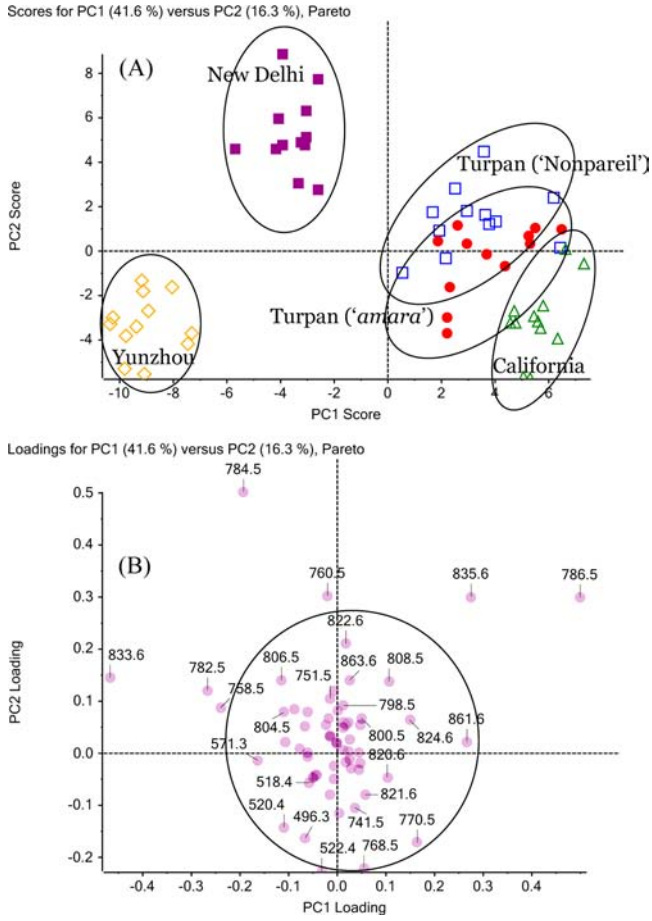

Figure 4. Principal component analysis of the identified phospholipid species of almond samples (A). Loading plot for the identified phospholipid species of almond samples (B).

833.6 to 835.6 was 1.07. However, the ratios of m/z 833.6 to 835.6 of Turpan 'Nonpareil' samples, Turpan '*amara*' samples, and California samples were 0.46, 0.46, and 0.47, respectively, indicating that these ratios could not be used as markers for differentiating these three samples. The results revealed that the ratio of m/z 833.6 to 835.6 could be used as a potential marker for distinguishing Yunzhou and New Delhi samples, but not as efficiently in the rest three batches. The ratio of $[PC36:3 + H]^+$ (m/z 784.5) to $[PC36:2 + H]^+$ (m/z 786.5) in the positive spectrum was agreed well with that of 833.6/835.6. Then, the mass range 810−830 was investigated, and a representative peak in all California almond samples was found. The ion at m/z 821.6 was tentatively attributed to $[PI O - 16:0/18:1 - H]^-$ (Figure 6A,B). Finally, the diagnostic ions for Turpan samples were also screened, but no satisfactory results were obtained, because the spectra of Turpan 'Nonpareil' sample and Turpan '*amara*' sample were generally the same, except that a diagnostic ion at m/z 571.4 ($[PI16:0 - H]^-$) was absent in 70% of Turpan '*amara*' samples. In brief, phospholipids have potential in tracking the geographical origins (Turpan, Yunzhou, New Delhi, and California) of almonds (*P. dulcis* L. cv Nonpareil), but do not as efficiently differentiate the almond cultivars or varieties, at least 'Nonpareil' and '*amara*', from the same area (Turpan). The reasons could be probably attributed to the unsaturation level of fatty acyl chains of phospholipids depending on the environmental conditions, such as temperature, pressure, and illumination. Using temperature as an

dx.doi.org/10.1021/jf4016448 | J. Agric. Food Chem. 2013, 61, 7739−7748

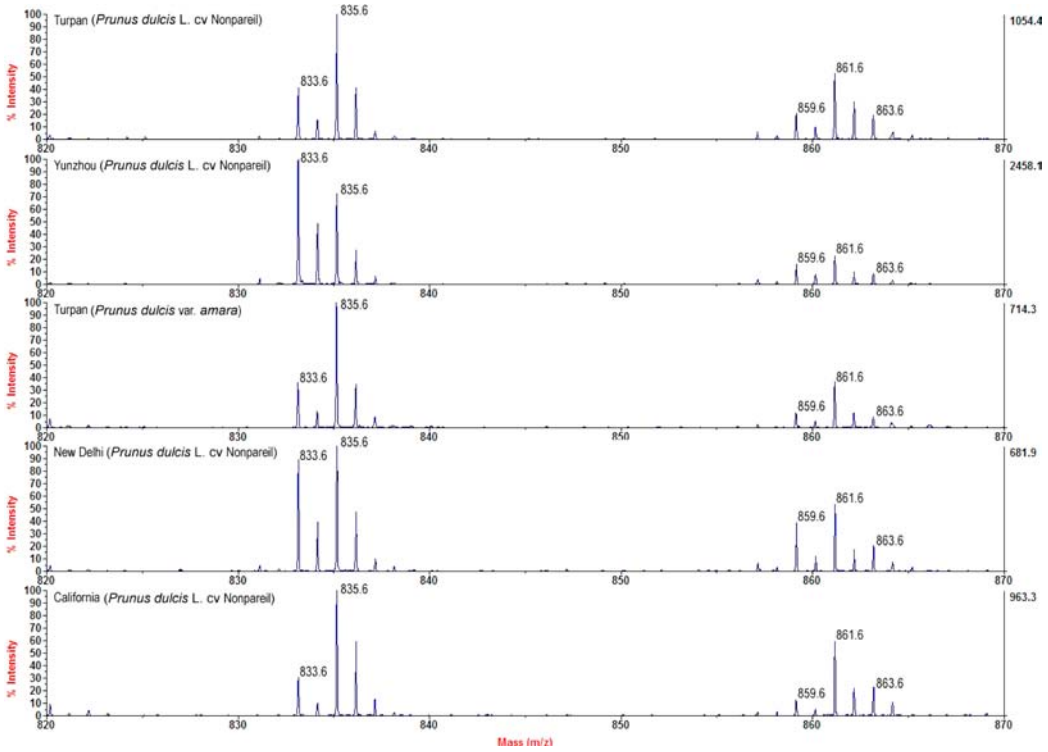

Figure 5. MALDI MS spectra (negative ion mode) in the *m*/*z* range 820−870 of five almond batches from four different geographical origins.

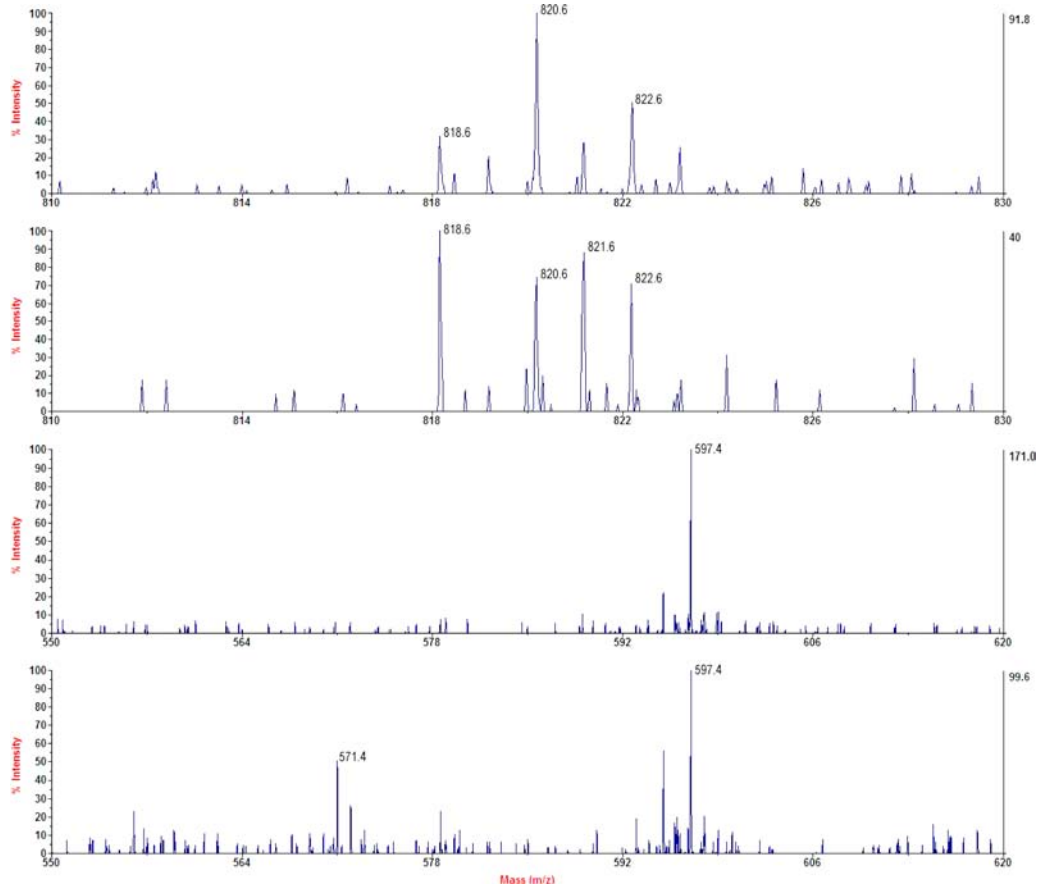

Figure 6. Expanded views of the *m*/*z* range 810−830 of almond samples from Turpan (A, top) and almond samples from California (B, second from top); expanded views of the *m*/*z* range 550−620 of *Prunus dulcis* var. *amara* (C, second from bottom) and *Prunus dulcis* L. cv Nonpareil (D, bottom).

dx.doi.org/10.1021/jf4016448 | J. Agric. Food Chem. 2013, 61, 7739−7748

example, almond cultivars growing in a colder locality showed a higher unsaturation level of fatty acyl chains of phospholipids. Turpan has very hot and long summers, and the almonds produced there, whether 'Nonpareil' or '*amara*', showed a low ratio of *m/z* 833.6/835.6. Southeastern California is an arid, hot desert, with routine extreme high temperatures during the summer, resulting in almonds there showing low unsaturation levels, also. On the contrary, Yunzhou has a pleasant climate, with an annual average temperature 5.5 °C, and the almonds cultured in Yunzhou had the highest ratio of *m/z* 833.6/835.6.

In summary, a TiO_2 NP based MSPD sample pretreatment procedure was developed to selectively extract phospholipids from almond samples, and MALDI-TOF/MS permitted a sensitive, fast, and efficient detection of the phospholipid species in both positive and negative ion modes. The PCA results indicated that the negative ion mode spectrum could be treated as a lipidomic fingerprint, and the ratio of 833.6/835.6 and the ion of 821.6 could be used as potential markers for differentiating the geographical origins (Turpan, Yunzhou, New Delhi, and California) of the tested almond batches (*P. dulcis* L. cv Nonpareil). An additional almond cultivar (*P. dulcis* var. *amara*) from Turpan was also tested. However, the results seem not satisfactory for distinguishing different almond cultivars ('Nonpareil' and '*amara*') from the same area.

AUTHOR INFORMATION

Corresponding Author

*(H.-Y. C.) Phone: +852 27887746. Fax: +852 27887406. E-mail: bhhonyun@cityu.edu.hk. (Z.Z.) E-mail: zhangzhf99@gmail.com.

Author Contributions

‖Q.S. and W.D. contributed equally to this work.

Funding

Our deep gratitude goes first and foremost to the Hong Kong Chinese Materia Medica Standards (HKCMMS) Fund (CityU Project 9211024) from the Department of Health, Hong Kong SAR Government, and the Internal Fund (No. 7002872) from the City University of Hong Kong. Also, Q.S., W.D., M.Y., and L.L. express their heartfelt thanks to the Research Grants Council (RGC) of Hong Kong in the City University of Hong Kong for financial support.

Notes

The authors declare no competing financial interest.

ABBREVIATIONS USED

PC, phosphatidylcholine; PE, phosphatidylethanolamine; PI, phosphatidylinositol; PA, phosphatidic acid; PG, phosphatidylglycerol; TiO_2 NPs, titanium dioxide nanoparticles; B&D, Bligh and Dyer; MALDI-TOF/MS, matrix-assisted laser desorption ionization−time-of-flight/mass spectrometry; PCA, principal component analysis

REFERENCES

(1) Kester, D. E.; Gradziel, T. M.; Grasselly, C. Almonds (*Prunus*). In *Genetic Resources of Temperate Fruit and Nut Crops*; Moore, J. N., Ballington, H. J., Eds.; International Society for Horticultural Science: Leuven, Belgium, 1991; pp 701−758.

(2) Schirra, M. Postharvest technology and utilization of almonds. *Hortic. Rev.* **1997**, *20*, 267−292.

(3) Socias i Company, R.; Kodad, O.; Alonso, J. M.; Gradziel, T. M. Almond quality: a breeding perspective. *Hortic. Rev.* **2008**, *34*, 197−238.

(4) Davis, P.; Iwahashi, C. K.; Yokahama, W. Whole almonds activate gastrointestinal tract anti-proliferative signaling in APCmin (multiple intestinal neoplasia) mice. *FASEB J.* **2003**, *17*, A1153.

(5) Haider, S.; Batool, Z.; Haleem, D. J. Nootropic and hypophagic effects following long term intake of almonds (*Prunus amygdalus*) in rats. *Nutr. Hosp.* **2012**, *27*, 2109−2115.

(6) Llorach, R.; Garrido, I.; Monagas, M.; Urpi-Sarda, M.; Tulipani, S.; Bartolome, B.; Andres-Lacueva, C. Metabolomics study of human urinary metabolome modifications after intake of almond (*Prunus dulcis* (Mill.) D.A. Webb) skin polyphenols. *J. Proteome Res.* **2010**, *9*, 5859−5867.

(7) Bolling, B. W.; Chen, C. Y. O.; McKay, D. L.; Blumberg, J. B. Tree nut phytochemicals: composition, antioxidant capacity, bioactivity, impact factors. A systematic review of almonds, Brazils, cashews, hazelnuts, macadamias, pecans, pine nuts, pistachios and walnuts. *Nutr. Res. Rev.* **2011**, *24*, 244−275.

(8) Bolling, B. W.; Dolnikowski, G.; Blumberg, J. B.; Chen, C. Y. O. Polyphenol content and antioxidant activity of California almonds depend on cultivar and harvest year. *Food Chem.* **2010**, *122*, 819−825.

(9) Kodad, O.; Estopanan, G.; Juan, T.; Company, R. S. Xenia effects on oil content and fatty acid and tocopherol concentrations in autogamous almond cultivars. *J. Agric. Food Chem.* **2009**, *57*, 10809−10813.

(10) Kodad, O.; Company, R. S. Variability of oil content and of major fatty acid composition in almond (*Prunus amygdalus* Batsch) and its relationship with kernel quality. *J. Agric. Food Chem.* **2008**, *56*, 4096−4101.

(11) Martín-Carratalá, M. L.; Llorens-Jordá, C.; Berenguer-Navarro, V.; Grané-Teruel, N. Comparative study on the triglyceride composition of almond kernel oil. A new basis for cultivar chemometric characterization. *J. Agric. Food Chem.* **1999**, *47*, 3688−3692.

(12) Prats-Moya, S.; Grané-Teruel, N.; Berenguer-Navarro, V.; Martín-Carratalá, M. L. Inductively coupled plasma application for the classification of 19 almond cultivars using inorganic element composition. *J. Agric. Food Chem.* **1997**, *45*, 2093−2097.

(13) Beltrán, A.; Ramos, M.; Grané, N.; Martín, M. L.; Garrigós, M. C. Monitoring the oxidation of almond oils by HS-SPME−GC−MS and ATR-FTIR: application of volatile compounds determination to cultivar authenticity. *Food Chem.* **2011**, *126*, 603−609.

(14) Sanahuja, A. B.; Moya, M. S. P.; Perez, S. E. M.; Teruel, N. G.; Carratala, M. L. M. Classification of four almond cultivars using oil degradation parameters based on FTIR and GC data. *J. Am. Oil Chem. Soc.* **2009**, *86*, 51−58.

(15) Sanahuja, A. B.; Teruel, N. G.; Carratala, M. L. M.; Selva, M. C. G. Characterization of almond cultivars by the use of thermal analysis techniques. Application to cultivar authenticity. *J. Am. Oil Chem. Soc.* **2011**, *88*, 1687−1693.

(16) Cullis, P. R.; de Kruijff, B. Lipid polymorphism and the functional roles of lipids in biological membranes. *Biochim. Biophys. Acta, Rev. Biomembr.* **1979**, *559*, 399−420.

(17) Calvano, C. D.; De Ceglie, C.; Aresta, A.; Facchini, L. A.; Zambonin, C. G. MALDI-TOF mass spectrometric determination of intact phospholipids as markers of illegal bovine milk adulteration of high-quality milk. *Anal. Bioanal. Chem.* **2013**, *405*, 1641−1649.

(18) Calvano, C. D.; Ceglie, C. D.; D'Accolti, L.; Zambonin, C. G. MALDI-TOF mass spectrometry detection of extra-virgin olive oil adulteration with hazelnut oil by analysis of phospholipids using an ionic liquid as matrix and extraction solvent. *Food Chem.* **2012**, *134*, 1192−1198.

(19) Wang, Y.; Zhang, H. Tracking phospholipid profiling of muscle from *Ctennopharyngodon idellus* during storage by shotgun lipidomics. *J. Agric. Food Chem.* **2011**, *59*, 11635−11642.

(20) Standal, I. B.; Axelson, D. E.; Aursand, M. ^{13}C NMR as a tool for authentication of different gadoid fish species with emphasis on phospholipid profiles. *Food Chem.* **2010**, *121*, 608−615.

(21) Shen, Q.; Wang, Y.; Gong, L.; Guo, R.; Dong, W.; Cheung, H. Shotgun lipidomics strategy for fast analysis of phospholipids in

fisheries waste and its potential in species differentiation. *J. Agric. Food Chem.* **2012**, *60*, 9384−9393.
(22) Boselli, E.; Pacetti, D.; Lucci, P.; Frega, N. G. Characterization of phospholipid molecular species in the edible parts of bony fish and shellfish. *J. Agric. Food Chem.* **2012**, *60*, 3234−3245.
(23) Pacetti, D.; Lucci, P.; Boselli, E.; Frega, N. G. Effect of antioxidant-enriched foods on plasma: phospholipid molecular species composition. *Eur. J. Lipid Sci. Technol.* **2009**, *111*, 1201−1211.
(24) Hankin, J. A.; Murphy, R. C. Relationship between MALDI IMS intensity and measured quantity of selected phospholipids in rat brain sections. *Anal. Chem.* **2010**, *82*, 8476−8484.
(25) Chen, S.; Li, K. W. Mass spectrometric identification of molecular species of phosphatidylcholine and lysophosphatidylcholine extracted from shark liver. *J. Agric. Food Chem.* **2007**, *55*, 9670−9677.
(26) Chen, S.; Belikova, N. A.; Subbaiah, P. V. Structural elucidation of molecular species of pacific oyster ether amino phospholipids by normal-phase liquid chromatography/negative-ion electrospray ionization and quadrupole/multiple-stage linear ion-trap mass spectrometry. *Anal. Chim. Acta* **2012**, *735*, 76−89.
(27) Frison, S.; Sporns, P. Variation in the flavonol glycoside composition of almond seedcoats as determined by MALDI-TOF mass spectrometry. *J. Agric. Food Chem.* **2002**, *50*, 6818−6822.
(28) Fretts, A. M.; Mozaffarian, D.; Siscovick, D. S. Associations of plasma phospholipid and dietary alpha linolenic acid with incident atrial fibrillation in older adults: the cardiovascular health study. *J. Am. Heart Assoc.* **2013**, *2*, 2047−9980.
(29) Sundström, B.; Johansson, G.; Kokkonen, H.; Cederholm, T.; Wallberg-Jonsson, S. Plasma phospholipid fatty acid content is related to disease activity in ankylosing spondylitis. *J. Rheumatol.* **2012**, *39*, 327−333.
(30) Qiao, L.; Roussel, C.; Wan, J.; Yang, P.; Girault, H. H.; Liu, B. Specific on-plate enrichment of phosphorylated peptides for direct MALDI-TOF MS analysis. *J. Proteome Res.* **2007**, *6*, 4763−4769.
(31) Calvano, C. D.; Jensen, O. N.; Zambonin, C. G. Selective extraction of phospholipids from dairy products by micro-solid phase extraction based on titanium dioxide microcolumns followed by MALDI-TOF-MS analysis. *Anal. Bioanal. Chem.* **2009**, *394*, 1453−1461.
(32) Engholm-Keller, K.; Larsen, M. R. Titanium dioxide as chemo-affinity chromatographic sorbent of biomolecular compounds applications in acidic modification-specific proteomics. *J. Proteomics* **2011**, *75*, 317−328.
(33) Harrabi, S.; Herchi, W.; Kallel, H.; Mayer, P. M.; Boukhchina, S. Liquid chromatographic-mass spectrometric analysis of glycerophospholipids in corn oil. *Food Chem.* **2009**, *114*, 712−716.
(34) Weihrauch, J. L.; Son, Y. S. The phospholipids content of foods. *J. Am. Oil Chem. Soc.* **1983**, *60*, 1971−1978.